INVESTIGATION ON PRECIPITATIONS AND DEFECTS OF THE Fe-24Cr-2Si-0.8Mn FERRITIC SUPER ALLOY STEEL

M. Dani[1], Parikin[1], R. Iskandar[2] and A. Dimyati[1]

[1]*Center for Science and Technology of Advanced Materials - National Nuclear EnergyAgency*
Puspiptek Area, Serpong 15314, Tangerang Selatan , Indonesia
[2]*Central Facility for Electron Microscopy (GFE), RWTH Aachen University*
Ahornstr.55,D-52074 Aachen, Germany
E-mail: mdani@batan.go.id

ABSTRACT

INVESTIGATION ON PRECIPITATIONS AND DEFECTS OF THE Fe-24Cr-2Si-0.8Mn FERRITIC SUPER ALLOY STEEL. A ferritic Fe-24Cr-2Si-0.8Mn alloy was produced from granular ferro-scrap, ferrochrome, ferrosilicon and ferromanganese in a conventional induction furnace. The alloy is dedicated for application as structure material in high temperature devices, such as nuclear reactor vessel and heat exchanger. The alloy has been verified to have high tensile strength and high resistant against corrosion. The aim of this work is to study the microstructures, chemical compositions and precipitation occurred inside grain and grain boundary of the alloy, to obtain more information of its superior physical-chemical properties. STEM-EDX mappings reveal the present of relatively large aluminum oxide, silicon carbide and high oxygen and high carbon containing precipitations on the specimens. The grains that were formed, exhibit relatively strong deformations as obviously shown by the elongated grains and sub-grains with typical high density of dislocations, even though, less mechanical treatments applied. Small porosities are also present homogeneously separated on the whole view area.

Keywords: Ferritic Fe-24Cr-2Si-0.8Mn alloy, FIB, SEM, TEM, EDX, STEM, HRTEM

ABSTRAK

INVESTIGASI TERHADAP PENGENDAPAN DAN KERUSAKAN PADA BAJA PADUAN *SUPER FERRITIC* Fe-24Cr-2Si-0,8Mn. Paduan Fe-24Cr-2Si-0,8Mn feritik dihasilkan dari granular *ferro-scrap*, *ferrochrome*, *ferrosilicon* dan *ferromanganese* dalam tungku induksi konvensional. Paduan ini didedikasikan untuk aplikasi sebagai bahan struktur pada perangkat suhu tinggi seperti bejana reaktor nuklir dan *heat exchanger*. Paduan telah diverifikasi memiliki kekuatan tarik tinggi dan tahan terhadap korosi. Tujuan dari penelitian ini adalah untuk mendalami strukturmikro, komposisi kimia dan presipitasi yang terjadi di dalam batas butir dan butir paduan, untuk mendapatkan lebih banyak informasi sifat fisik-kimia superior. Pemetaan *STEM-EDX* mengungkapkan adanya oksida aluminium yang relatif besar, silikon karbida dan oksigen tinggi dan presipitasi tinggi yang mengandung karbon pada spesimen. Butiran yang terbentuk, menunjukkan deformasi yang relatif kuat seperti yang ditunjukkan oleh butiran dan sub-butiran memanjang dengan kepadatan dislokasi yang khas, walaupun sedikit mendapat perlakuan mekanik. Porositas kecil juga berada secara merata terpisah pada keseluruhan daerah yang diamati.

Kata kunci: Paduan Feritik Fe-24Cr-2Si-0.8Mn, *FIB, SEM, TEM, EDX, STEM, HRTEM*

INTRODUCTION

National Nuclear Energy Agency plans to build an experimental power reactor with a capacity of 10 MWth. The reactor to be used is the type of gas reactor with a high operating temperature (High Temperature Gas Cooled Reactor- HTGR). In addition to the electrical energy, the heat energy from coolant gas can still be used for industrial processes. It can be expected total efficiency of the HTGR can be higher than conventional power reactor systems. For the selection of materials suitable for the physical condition of the entire system of heat transfer from the reactor vessel, heat exchanger pipeline is crucial to the efficiency that can really be achieved this power reactors. The main reason behind the synthesis of corrosion-resistant stainless-steel alloys is the fact that the alloy must be resistant to corrosive environment. One of the requirements for reactor structural materials, particularly vessel and heat exchanger is that the material must be resistant to corrosion caused by the environment. As a rule, a stainless-steel alloy would contain the one basic alloying element, namely a minimum of 10.5% chromium; this ferritic stainless-steel Fe-24Cr-2Si-0.8Mn alloy include in high chromium ferritic stainless steel classification that usable in wide range of application [1-2].

Because of its superior properties, ferritic steels containing high chromium is a material that is generally used as a structural material in nuclear reactor technology, for which the very popular example are the SS304 and AISI430 commercial steels. These steels have a primary alloying element of chromium between 12 to 30 % and the carbon content is so low. The alloy has the corrosion resistance to high temperatures (> 500 ° C). At room temperature, this steel alloy forms α-Fe-Cr with a body-centered cubic crystal structure (BCC). While the other requirement is that a structural material must be withstand to the mechanical loads, to temperature load, and resistant to neutron irradiation [3].

On the other hand, within the framework of advanced materials research program, Indonesian National Nuclear Energy Agency has synthesized ferritic Fe-24Cr-2Si-0.8Mn alloy using local raw material [4]. Now, this ferrite material has been independently fabricated in the authors' own laboratory. In this work, the super ferritic stainless steel made from the granular ferro-scrap, ferro-chrome, ferro-manganese, and ferro-silicon with small addition of titanium by melting method. From preliminary research, it is found that the Fe-24Cr-2Si-0.8Mn alloy exhibits high material hardness and good weld capability [3,6].

The purpose of this study is to characterize the microstructure of the experimental ferritic Fe-24Cr-2Si-0.8Mn steel, especially in accordance to its corrosion resistance. Then, the results were analyzed, discussed and compared with each other to assess some advantages of the Fe-24Cr-2Si-0.8Mn steel as reactor structure material. Characterization was performed using methods and techniques that evolved in the actual SEM and TEM technology today.

Precipitation is the most important factor for the formation of mechanical properties at high temperatures. Formation, dissolution and coarsening of precipitates must be understood for example to achieve good creep properties [7]. Type, morphology, size distribution and stability of precipitates are factors dominating the creep behavior of the alloy. The precipitation of secondary phases and the development of the matrix in the steel during tempering will determine the properties of the steels [8].

The aim of this research is to study the microstructures and chemical compositions of the matrix and precipitationsoccurred inside grain and grain boundary of the alloy, to obtain more information of its superior physical-chemical properties.

EXPERIMENTAL METHOD

Materials and Method

Materials used in this work is the ferritic Fe-24Cr-2Si-0.8Mn steel with the chemical composition (wt%) as shown in Table 1, measured with optical emission spectrometry (OES) in Polman Bandung. Super ferritic alloy Fe-24Cr-2Si-0.8Mn is a new ferritic type contains high chromium element and additional, silicon and carbon. Other elements as well as Ti addition give a relatively better pitting corrosion due to reduced segregation [9-12], whereas phosphor and sulphur elements are assumed to be impurities from the raw materials; the composition is listed in Table 1 below [13]. The specimen was synthesized by casting methods in an induction furnace at Telimek LIPI Bandung.

JEOL scanning electron microscopes, JSM 6510LA and JSM 7000F, were used for chemical and surface morphology analysis of the bulk specimen. SEM image is recorded using secondary electron detector (SE) at the acceleration energy of the primary electron beam

Table 1. Elements composition in super ferritic alloy Fe-24Cr-2Si-0.8Mn as a result of spark errosion optical emission spectroscopy (OES).

Element	%wt
Fe	72.97
Cr	23.71
Si	2.02
Mn	0.821
C	0.258
Ni	0.12
P	0.023
S	0.015
Al	0.007
Ti	0.006

source tungsten wire by a maximum of 20 keV with a working distance or WD kept constant at 10 mm. WD value is setup to get EDX spectrum in the best condition. EDX taken on the value of dead time on average between 20% to 40%. More detailed information has been discussed in previous publications [14]. TEM lamella was prepared by means of focused ion beam technique (FIB) using FEI Strata 205. The TEM/STEM analysis were performed on a Schottky emission Zeiss Libra 200 FE equipped with in column corrected omega filter. The HAADF signal and EDS mapping were acquired by using Fishione HAADF detectors and X-Flash from Bruker respectively.

RESULTS AND DISCUSSION

The results of the SEM observation on the polished sample of the Fe-24Cr-2Si-0.8Mn steel with magnification of 600x can be seen in Figure 1 and corresponding EDX measurements are presented in Figure 2. It is obvious that the Fe-24Cr-2Si-0.8Mn sample is a type of ferritic steel, due to its alloy composition lack of the Ni elements and a predominance of Cr element. However, small voids are homogenously distributed across on the entire observed area. Some large precipitates are also found, which are surrounded by porosity at their boundaries. From the sample matrix no.001, it can be concluded that the sample matrix contains Si and Mn, which are assumed to be the reason of its high resistant against wet corrosion as previously reported in [3,15,16].
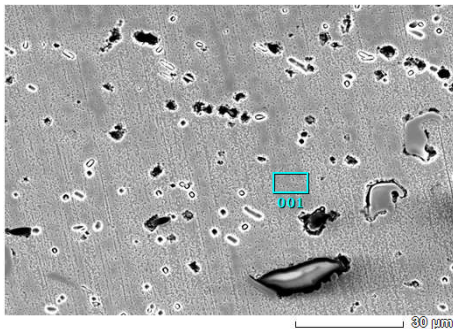

Figure 1. SEM image of the Fe-24Cr-2Si-0.8Mn sample

Figure 2(b) shows EDX spectrum on a precipitate indicated by number 002 on the SEM image in Figure 1. The chemical composition consisting of Mn, Cr, Si and Al that are mainly occur as metal oxides is obtained. This observation stands in agreement with the results of Effendi's measurement as reported in [13,17]. Otherwise, precipitates indicated in Figure 2c are identified as chromium carbide ($Cr_{23}C_6$), reported by Parikin et.al. [18].

Figure 3 shows the SEM image of the sample in cross-section view. High deformation presents in upper part of the sample, which is occur possibly due to the machining process during grinding [18]. In upper line of
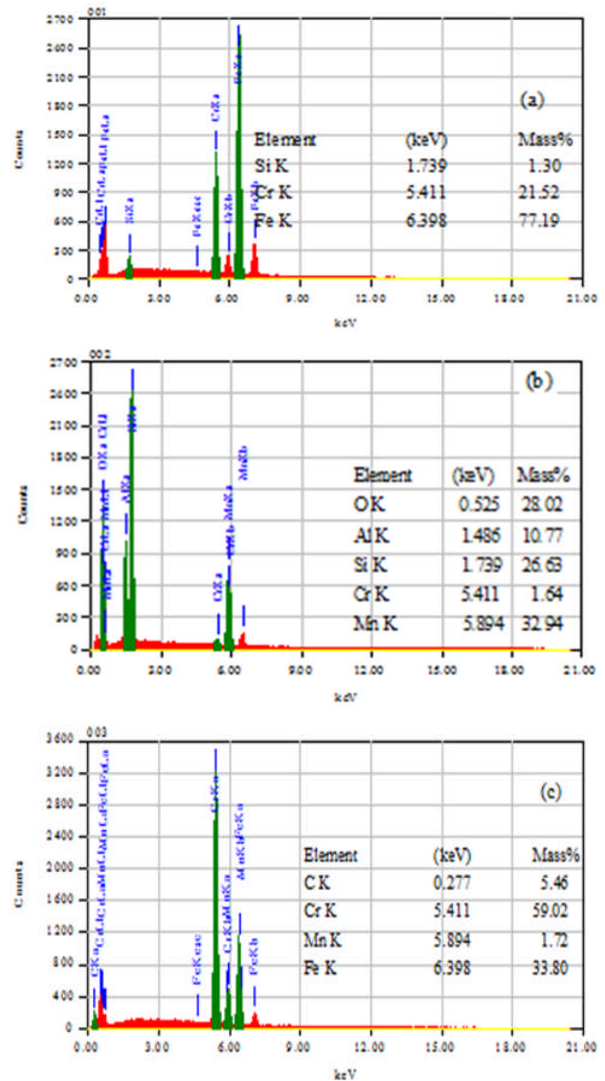

Figure 2. EDX results on sample area as indicated in Figure 1 (a) matrix (b) precipitate 002 and (c) precipitate 003

Figure 3. SEM image of the sample cross-section with magnification of 3300 x.

the surface, cracking and coarse clusters spread clearly as black spots. Clearly, other than due machining process also the casting process was less than perfect so the slugs still are covering most of the surface of the material. In Figure 4 is STEM image on the lamella in dark field

175

mode taken from the area marked by the rectangular in Figure 3. It can be seen clearly the texture microstructure on the top and different grain sizes at the area about 10 mm beneath the surface. Differences clots of the grains that form alloy clearly visible such as rocks pearl in the real world. Beautiful strands of white, black and gray rocks look like coiled around the axis of the matrix grains.
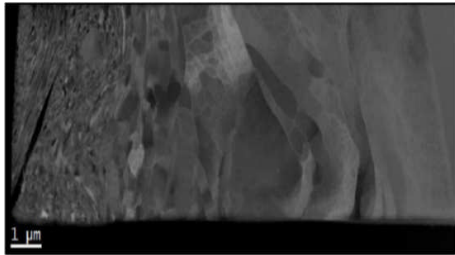

Figure 4. The STEM-DF image of a lamella prepared on area marked on Figure 3.

Figure 5 shows more detail analysis at higher magnification that were performed on STEM imaging. It was revealed that deformations occurred in the form of line dislocations (see dent lines on the matrix surfaces). These deformations also consist of different grains morphology located up to 1.7 µm below the surface. This would be caused by different heat dissipation during the machining process. The heat dissipation that is released when there are a lot of friction with the machining tools. TEM [19-20] bright-field image analysis shows the matrix contains high deformations and defects (see Figure 5). It concentrates at matrix-precipitates grain boundary, which was due to internal stress during the precipitates formation. It can be seen that nano-pores was formed on this region also, due to failure in cooling trap.
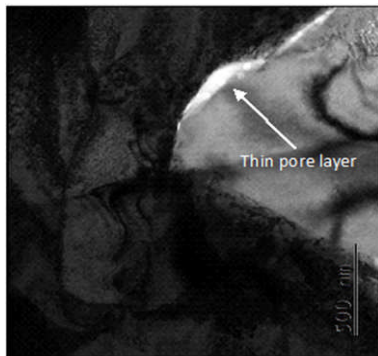

Figure 5. A magnification 9×10^4 x of STEM bright-field image of precipitate formed close to surface area. A very thin poreslayer also detected at precipitate in the matrix interface.

Moreover, the phase and chemical analysis were done to see the phase present on the specimen [20-22] (Figure 7). Figure 7 (a) shows the STEM-ADF image of the same precipitation of Figure 6. The spot diffraction (inset) is corresponding to Selected Area Electron Diffraction (SAED) pattern, which shows that the matrix identified as Fe0.8Cr0.8 phase [19-21]. Deviation on lattice
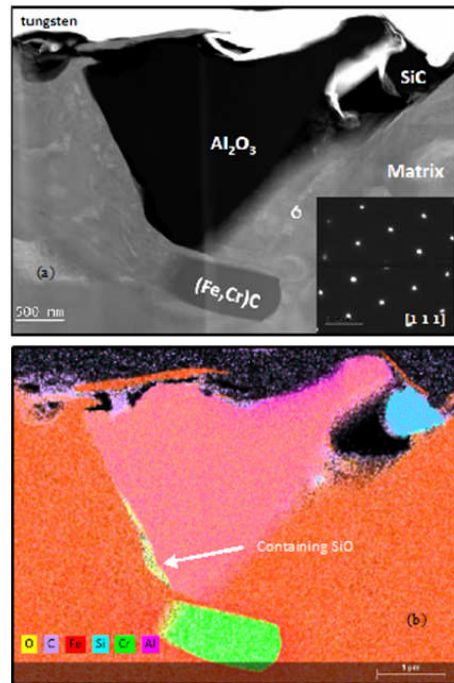

Figure 6. (a) STEM-ADF and (b) EDX elemental map show the presence of precipitates formation on the specimen.

parameters was also detected that indicate the possibility for silicon and manganese atoms substitution. This identified from the blur and bright spots of the SAED-diffraction in inset Figure 6 (a). Mixture precipitates were detected from EDS map in Figure 6 (b). Oxides and carbides, probably Al_2O_3 and SiC, were formed at area close to the surface and (Fe,Cr)C formed at deeper location. Furthermore, EDX map shows also a
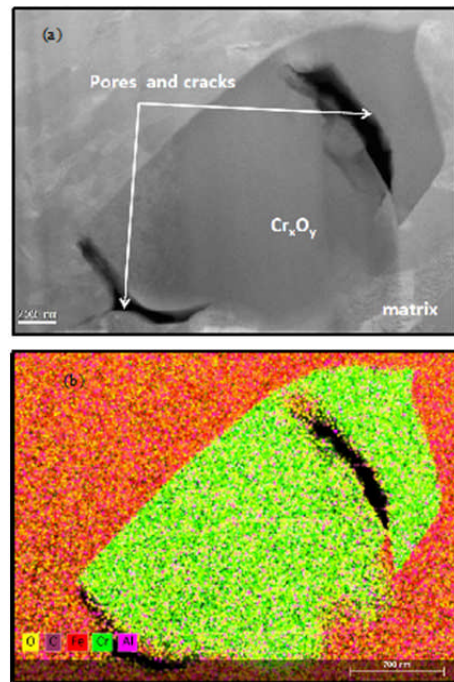

Figure 7. (a) STEM-ADF and (b) EDX map show the chromia precipitate with sub-micron pores and cracks.

very thin SiO layer, about 100 nm thick, formed at the Al_2O_3 – matrix interface. Experimental pattern, taken from the matrix area, has been index as [111] and has the best fit with simulated pattern from crystallography database Fe0.8Cr0.2 (reg – Nr: 102752). Slightly mismatch due to variation concentration between Fe and Cr (based on EDX).

High-resolution imaging technique was also performed to have more detail information of the defects formed at the specimen. As can be seen in Figure 6 (a), at the matrix area where is sandwiched by two precipitates, Al_2O_3 and (Fe,Cr)C, high concentration impurities were detected. Parikin et. al. [18] reported that some impurities in which detected by using neutron diffraction technique are indicated: $Al_2O_3.54SiO_2$, Al_4C_3, $Cr_{23}C_6$ and SiC, appearing as weak peaks. Higher magnification image of selected area shows also dislocation present at the Al_2O_3 matrix interface. So, the figure gives absolutely a conformation of the obtained data, especially for alumina, silicon oxide and chrome carbide.

High-resolution imaging technique was also performed to have more detail information of the defects formed at the specimen. As can be seen in Figure 6 (a), at the matrix area where is sandwiched by two precipitates, Al_2O_3 and (Fe,Cr) C, high concentration impurities were detected. Parikin et. al. [18] reported that some impurities in which detected by using neutron diffraction technique are indicated: Al_2O_3. $54SiO_2$, Al_4C_3, $Cr_{23}C_6$ and SiC, appearing as weak peaks. Higher magnification image of selected area shows also dislocation present at the Al_2O_3 matrix interface. So, the figure gives absolutely a conformation of the obtained data, especially for alumina, silicon oxide and chrome carbide.

The presence of cracks on the precipitates was also detected in the surface. As can be seen on Figure 7 and Figure 8, the sub-micro pores formed on interface of chromia precipitate. Higher magnification image of selected area shows also dislocation present at the Al_2O_3 matrix interface.
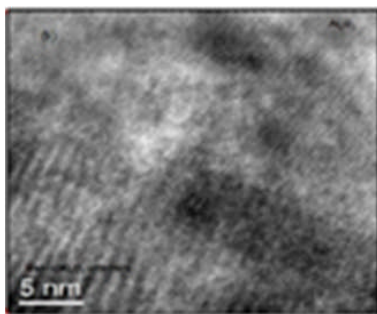

Figure 8. HRTEM image shows the precipitates matrix interface area.

CONCLUSSION

We have shown in this work that a Ferritic alloy steel was successfully synthesized from ferro-scrap, ferrochrome, ferrosilicon and ferromanganese using

Induction Furnace. STEM analysis founds high deformation formed at the near surface which is probable due to the machining process. The STEM-EDX combined with SAED analysis were successfully identified Al_2O_3, Cr_2O_3, Fe-Cr-C and Si-C precipitates in the alloy. Detail chemical analysis suggested that mixture precipitates, which mainly oxides, only formed at area close to the surface area. SEM investigation founds some chromium and manganese oxides on the surface of the material. The existence of defects in the material will interfere with the strenghts of the material at high temperatures, so the next activity to be able to minimize the presence of these defects.

REFERENCES

[1]. K. A. Cashell, N. R. Baddo. "Ferritic Stainless Steel in Structural Applications." Thin-Walled Structures, vol. 83, pp.169-181. 2014.

[2]. V Geanta, I Voiculescu, E-M Stanciu. "Hafnium influence on the Microstructure of FeCrAl Alloys" IOP Conf. Series: Material Science and Engineering vol. 133, pp.1-8. 2016.

[3]. T. Darwanto and A.K. Jahja. "Micro- and Crystal Structure Analysis of New Ferritic Steel." Jusami, Indonesian Material Science Journal, vol. 11, no. 3, pp. 202-206. 2010.

[4]. A.K. Jahja. "Ferritic Stainless Steel Synthesis From Mining Materials." Proceedings of the ICMST 2010, 2010, pp 61-68.

[5]. N. Effendi and A.K. Jahja. "Structural Characterization and Its Physical Properties of Non-Standard A1 Austenite Steel." Int. Journal of Materials and Mechanical Engineering, vol. 3, no. 2, pp. 38-44. 2014.

[6]. Tri Darwinto, Parikin and Nurdin Effendi. "Corrosion Experiment on Standard Ferritic Steel F1 in Sea Water Medium." Seminar Nasional Teknologi Energi Nuklir, 15-16 Oktober 2015.

[7]. T. Sourmail. "Precipitation in Creep Resistant Austenitic Stainless Steels." Materials Science and Technology, vol. 17. 2001.

[8]. Cai, G.J., Andren, H.O., Svensson, F.L.E.,. "Microstructural Change of a 5% Cr Steel Weld Metal During Tempering". Mater. Sci. Eng. A, vol. 242, pp. 202-209. 1998.

[9]. G. Mallailah, P.Ravinder Reddy, A. Kumar. "Influence of Titanium Addition on Mechanical Properties, Residual Stresses, and Corrosion Behavior of AISI-430 Grade Ferritic Stainless Steel GTA Welds." Procedia Materials Science 6, pp.1740-1751. 2014.

[10]. C.H. Hsu, C.K. Lin, K.H. Huang, K.L. Ou. "Improvements on Hardness and Corrosion Resistance of Ferritic Stainless Steel Via PVD (Ti, Cr) N Coatings, Surface and Coatings Technology." vol. 231, pp.380-384. 2013.

[11]. Azim Safikhani, Mohammad Aminfard. "Effect of W and Ti Addition Oxidation Behavior and Area Specific Resistance of Fe-22Cr-0.5Mn Ferritic Stainless Steel for SOFCs Interconnect." International Journal of Hydrogen Engineering. vol. 39, pp.2286-2296. 2014.

[12]. M.P. Short, R.G.Ballinger, H.E. Hanninein. "Corrosion Resistance of Alloys F91 and Fe-12Cr-2Si in Lead–bismuth Eutectic upto 715°C." Journal of Nuclear Materials. Vol. 434, pp.259-281. 2013.

[13]. Nurdin Effendi. "Austenitic Stainless-Steel Production by Foundry." Urania, vol. 16, no. 2, pp. 69-77. 2010.

[14]. A. Sujatno, R. Salam, B. Bandriyana,A. Dimyati, Studi Scanning Electron Microscopy (SEM) untuk Karakterisasi Proses Oksidasi Paduan Zirkonium, Pros. Sem.Nas. X, SDM Teknologi Nuklir, 2014.

[15]. M. Dani, P. Untoro, T.Y. S. P. Putra, Parikin, J. Mayer and A. Dimyati. "TEM Characterization of High-Temperature Oxidation of Fe-20Cr-5Al Alloy Prepared by FIB Technique." Makara Journal of Technology; vol. 19, no. 2, pp. 85-9. 2015.

[16]. I. Wahyono, R. Salam, A. Dimyati, Parikin. "Characterization of Microstructures by Using SEM and XRD on Corrosion Resistant of SS430 Commercial Steel and F1 Non-Commercial Steel." Prosiding Seminar Nasional XI SDM Teknologi Nuklir, pp 112 – 117. 2015.

[17]. N. Effendi, T. Darwinto, A.H. Ismoyo and Parikin. "24-Chromium Ferritic Steel Magnetic Properties." Jurnal Sains Materi Indonesia, vol. 15, No. 4, pp. 187-191, 2014.

[18]. Parikin, M. Dani, A.K. Jahja, R. Iskandar and J. Mayer, "Micro-Crystal Structures Investigation on 73Fe24Cr2Si0.8Mn0.1Ni Ferritic Steel for Structure Material Applications." Int. J. of Tech., pp. 851, 2017.

[19]. K .Kanthavela, K. Arunkumar and S.Vivek. "Investigation of Chill Performance In Steel Casting Process Using Response Surface Methodology." Procedia Engineering, vol. 97, pp. 329 -337. 2014.

[20]. H. J. Kim, S. H. Choi, H.B. Bae and T. W. Lee. "Transmission Electron Microscopy (TEM) Sample Preparation of $Si_{1-x}Ge_x$ in c-Plane Sapphire Substrate." NASA STI Program, pp.1-39, August 2012.

[21]. K.A. Terrani, B.A. Pint, Y.-J., K.A. Unocic, Y. Yang, C.M. Silva, H.M. Meyer III, and R.B. Rebak. "Uniform Corrosion of FeCrAl Alloys in LWR Coolant Environment." Journal of Nuclear Material, vol. 479, pp.36-47, 2016

[22]. T.L. Burnett, R. Kelley, B. Winiarski, L. Contreras, M. Daly A. Gholinia M.G. Burke, and P.J. Withers. "Large volume serial section tomography by Xe Plasma FIB dual beam microscopy." Ultramicroscopy, Vol. 161, pp. 119-129. 2016.